

Exciton Binding Energy of Monolayer WS₂

Bairen Zhu⁺, Xi Chen⁺, Xiaodong Cui^{1, *}

¹*Department of Physics, The University of Hong Kong, Hong Kong, China*

(Dated: September 3, 2018)

The optical properties of monolayer transition metal dichalcogenides (TMDC) feature prominent excitonic natures. Here we report an experimental approach toward measuring the exciton binding energy of monolayer WS₂ with linear differential transmission spectroscopy and two-photon photoluminescence excitation spectroscopy (TP-PLE). TP-PLE measurements show the exciton binding energy of $0.71 \pm 0.01 \text{eV}$ of the band-edge excitons around K valley in the Brillouin zone.

PACS numbers: 78.66.-w 73.22.-f 78.20.-e 78.67.Pt

Coulomb interactions are significantly enhanced in low dimensional systems as a result of spatial confinement and reduced screening, and consequently excitons, quasi-particles of electron-hole pairs bounded by Coulomb force play a pronounced role in their optical aspects. A few paradigms of the pronounced excitonic effects have been demonstrated in quantum dots and carbon nanotubes where the exciton binding energies are found to be a fraction of their band gaps in these quasi-zero dimensional (0D) and one dimensional (1D) systems. Prominent exciton effects are also widely expected in intrinsic 2D systems for instance monolayer crystals of transition metal dichalcogenides (TMDC) owing to the reduced dielectric screening and spatial confinement[1, 2]. Monolayer TMDC is an intrinsic 2D crystal consisting of two hexagonal planes of chalcogen atoms and an intermediate hexagonal plane of metal atoms in a prismatic unit cell. Particularly MX₂ (MoS₂, MoSe₂, WS₂ and WSe₂) experiences a transition from indirect gap in bulk form to direct gap of visible frequency in monolayers, where the band gap is located at K(K') valley of the Brillouin zone[3–6]. Ab initio calculations show the direct-gap exciton binding energy in the range of 0.5-1eV which is around 1/3-1/2 of the corresponding optical direct gap[1, 2, 7, 8]. The modulated absorption/reflection spectroscopy shows the binding energy of direct gap excitons around 55meV in bulk crystals[10]. Such a big exciton binding energy in bulk form guarantees the robust excitonic nature of optical properties in ultrathin counterparts. Furthermore, photoluminescence (PL) experiments identify electron(hole)-bounded excitons, so called trions, with a charging energy E_{bX} of 18meV, 30meV and 20-40meV in monolayer MoS₂, MoSe₂ and WS₂ respectively[9, 11, 12]. With a simple 2D exciton model, one could estimate the exciton binding energy around 10 times that of the trion, if equal effective electron's and hole's mass are assumed[13]. As yet the direct measurement of exciton binding energy in monolayer TMDC is lacking.

Here we report experimental approaches toward measuring the exciton binding energy of monolayer WS₂ with linear differential transmission spectroscopy and two-photon photoluminescence excitation spectroscopy (TP-

PLE). The TP-PLE resolves the excited states of excitons and the interband transition continuum. The exciton binding energy of $0.71 \pm 0.01 \text{eV}$ of the band-edge excitons around K valley in the Brillouin zone is extracted by the energy difference between the ground state exciton and the onset of the interband continuum.

Monolayer WS₂ was mechanically exfoliated from single crystal WS₂ and identified with optical microscope and photoluminescence spectroscopy (supplementary information). The samples in differential transmission measurements were made by transferring from silicon substrates to freshly cleaved mica substrates as described in Ref[14]. The electric gate dependent PL measurements were carried out with a field effect transistor structure on silicon wafers with a 300nm oxide cap layer. The TP-PLE spectroscopy was carried out with a confocal setup with a 20X achromatic objective and a Ti:sapphire oscillator (80MHz, 100fs).

Figure 1a summarizes linear optical measurements of monolayer and multilayer WS₂. There are distinct peaks in the differential transmission spectra, labeled as “A”, “B” and “C” respectively[6, 10]. Peaks “A” around 2eV and “B” around 2.4eV at room temperature present the excitonic absorptions at the direct gap located at K valley of the Brillouin zones. The separation between “A” and “B” of 0.38eV rising from the splitting of valence band minimum (VBM) due to spin-orbit coupling (SOC) at K(K') valley is almost constant in all the layers with various thickness, consistent with the PL spectra[5, 6]. It is the direct result of the suppression of interlayer coupling at K(K') valley owing to the giant SOC and spin-valley coupling in tungsten TMDC with 2H stacking order in which each unit layer is a π rotation of its adjacent layers[5]. The peak “C” around 2.8eV was recognized as the excitonic transitions from multiple points near Γ point of the Brillouin zone[2, 10]. Unlike in many semiconductors, the linear absorption spectra of WS₂ display no gap between distinct excitons and the continuum of interband transitions. The continuous absorption originates from the strong electron(hole)-phonon coupling in TMDCs and the efficient phonon scattering fills the gap between the ground state excitons and the interband continuum in the linear absorption spectra[2]. As the tem-

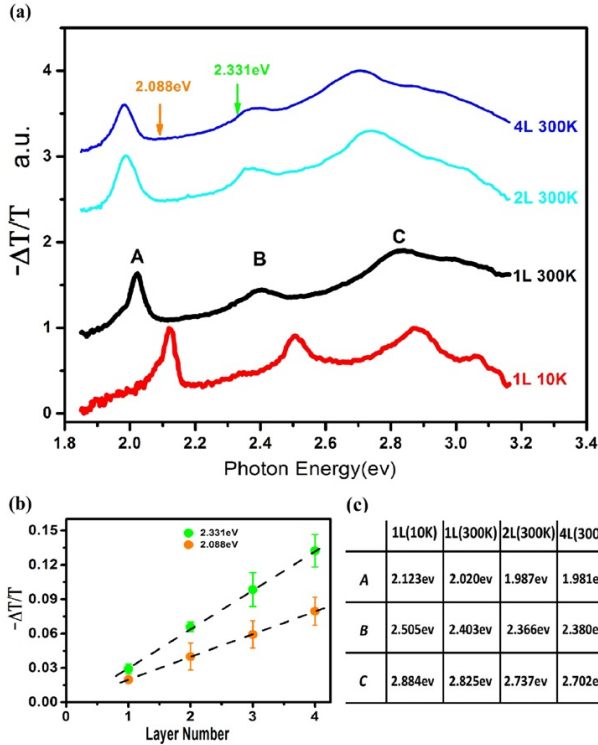


Figure 1: Linear absorption spectra of WS₂ atomically thin films. (a) Normalized differential transmission spectra of multi- and monolayer WS₂ at room temperature and 10K. (b) Absorbance of atomically thin layer at photon energy of 2.088eV (orange) and 2.331eV (green) respectively as indicated by arrows in figure 1(a). The absorbance shows a linearly dependence on layer number, each unit layer with constants of 2.0% and 3.4% respectively. (c) Absorption peak energy values of exciton “A”, “B” and “C”.

perature drops to 10K, the peak “A” and “B” are both blue-shifted by around 0.1eV and peak “C” is shifted by 0.06eV as shown in Figure 1c. The difference of the blue-shift is the direct consequence of the diverse locations of the excitons in the Brillouin zone: exciton “A” and “B” are formed at K valley while “C” is around Γ point. Nevertheless, the continuous absorption still survives and no distinct single-particle band edge emerges at cryogenic temperature (10K). The linear absorption spectra cannot resolve the exciton binding energy.

Figure 1b shows the absorbance of WS₂ atomically thin films as a function of the thickness above their ground exciton energy, which is approximated with the differential transmission. The absorbance of monolayer and multilayers is linearly proportional to their thickness, each layer absorbing around 2.0% and 3.4% at excitations of 2.088eV and 2.331eV respectively. The linear layer dependence of the absorption gives an experimental evidence of the suppression of interlayer hopping in 2H stacked WS₂ as a result of spin-valley coupling[5, 18]. The thickness dependence could also be used as a thick-

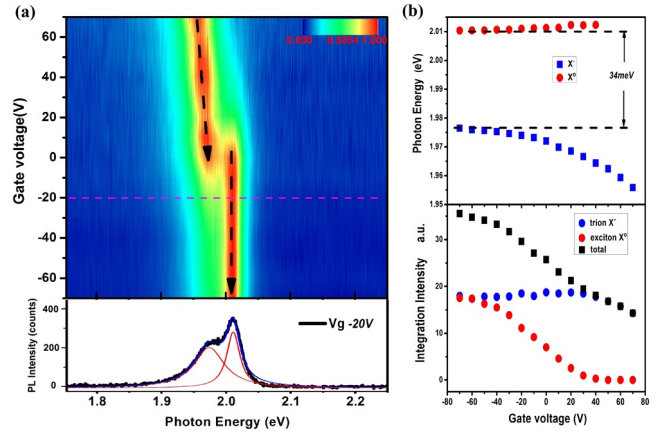


Figure 2: Electric doping dependent PL spectra at room temperature. (a) Colour contour plot of normalized PL spectra excited by a cw laser (2.331eV) under various back-gate bias. Dashed black arrows contour PL peaks of free exciton and trion states. Even at zero gate bias the trion X⁻ exists due to defects or substrate interactions. Fig. 2(b) illustrates the PL profile at V_g = -20V (dashed line labelled in the top panel) as a superposition of two Lorentzian shape lines in red. (c) Electric gating dependence of excitons’ and trions’ energies (upper panel) and the corresponding integrated intensities (bottom panel).

ness monitor for multilayer/monolayer characterization. There is a side bump at the red side of exciton A, which modifies the lineshape away from the symmetric Lorentzian or Gaussian shape. We tentatively attribute the bump to the effect of electron/hole bound exciton or trion[9, 11, 12]. Although the monolayer WS₂ is not intentionally doped, the structural defects and substrate effects such as charge transfer and defects modulate the carrier density away from its insulating state. To confirm the origin of the bump around exciton A, we record the PL spectra of monolayer WS₂ at various electric gating (from 70V to -70V) which continuously tunes the Fermi level of monolayer WS₂ as illustrated in figure 2a.

There is a prominent peak X⁻ at the red side of the free exciton X⁰ at V_g ≈ -20V and the PL spectrum could be described by a superposition of two Lorentzian curves which center at peak X⁰ and X⁻ respectively as illustrated in figure 2b. As the gate voltage goes towards positive values (V_g > 0), the free exciton X⁰ gradually diminishes and disappears at V_g > 40V. Meanwhile the red-side X⁻ rises to take over the overwhelming weight of the whole PL until starts to decrease at V_g > 20V probably due to the electrostatic screening effect[19], and the peak X⁻ is further red-shifted. The electric gating dependence attributes X⁻ to n-type trion (electron-bounded exciton) states. As V_g goes to negative bias, the free exciton state X⁰ takes over the weight of the PL and tends to saturate around V_g = -70V. While the trion state X⁻ monotonically diminishes, the redshift also shows a sign of saturation

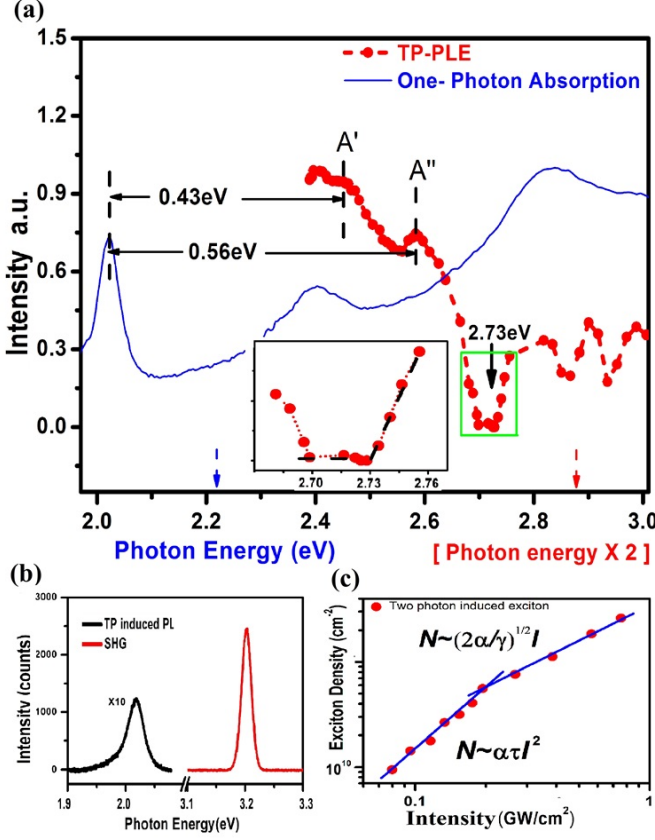


Figure 3: (a) One-photon absorption spectrum (blue) in visible range and two-photon photoluminescence exciton spectrum (red) with the excitation in the range of 1.192~1.5eV where the x axis presents the exciton energy (in blue) for linear absorption and the double of the excitation energy (in red) for TP-PLE. A' and A'' denote the excited states of exciton A and the zoom-in of the gap state section is shown in inset. The TP-PL intensity linearly increases with the excitation energy just above the threshold of the interband continuum, presenting the signature of two-photon process in 2D systems where the polarization sits in the 2D plane. (b) The spectra of TP-PL and the second harmonic generation (SHG) at the excitation of 1.6eV. The integrated intensity of the PL is more than one order of magnitude less than that of the SHG. (c) The intensity of ground state exciton *vs.* the excitation intensity under the excitation of 1.59eV. The fitting lines demonstrate a quadratic- (under low intensity) and a linear-dependence (under high intensity) respectively, which yield the exciton-exciton annihilation rate $\gamma \approx 0.31 - 0.47 \text{ cm}^2/\text{s}$ and the two-photon absorption cross section $\alpha \approx 3.5 - 5.3 \times 10^4 \text{ cm}^2 \text{ W}^{-2} \text{ S}^{-1}$.

of -34meV at around $V_g = -70\text{V}$. This confirms the trion (electron-bound exciton) origin of the side bump around exciton A in the monolayer transmission spectrum and the trion binding energy of 34meV in monolayer. If we follow the simplified trion model in conventional quantum wells[13] and take the effective mass of either $m_e = 0.37$ and $m_h = -0.48$ [20] or $m_e = 0.27, m_h = -0.32$ [7], the binding energy of free exciton is estimated at $E_b \approx 0.1\text{eV}$.

Two-photon excitation is a third order optical process involving simultaneous absorption of the two photons which follows selection rules different from those in one-photon (linear) process. As a photon has an odd intrinsic parity, one- and two-photon transitions are mutually exclusive in systems with inversion symmetry: one-photon transitions are allowed between states with different parity and two-photon transitions between states with the same parity; in systems without inversion symmetry like monolayer TMDCs described by a point group of D_{3h} symmetry, parity is not a good quantum number and there exist transitions which are both one- and two-photon allowed. Nevertheless, the oscillator strengths of exciton states are generally different between one- and two-photon processes. A simplified exciton model could be described as $U_n^l(\rho = r_e - r_h)\phi_c(r_e)\phi_v(r_h)$ where $\phi_c(r_e)(\phi_v(r_h))$ presents the electron (hole) wave function, and U_n^l is the function of relative motion of electron-hole. The optical transition rates for one- and two-photon processes[15]

$$W_{OP} \sim |A|^2 \sum_{c,v} |\langle c | \varepsilon \cdot p | v \rangle|^2 \sum_{c,v} |\langle \phi_c | \phi_v \rangle|^2 \cdot |U_n^l(\rho = 0)|^2 S_{cv}(\hbar\omega)$$

$$W_{TP} \sim |A_1 A_2|^2 \sum_{c,v} |\langle c | \varepsilon \cdot p | v \rangle|^2 \sum_{c,v} |\langle \phi_c | \phi_v \rangle|^2 |\nabla U_n^l(\rho = 0)|^2 S_{cv}(\hbar\omega_1 + \hbar\omega_2)$$

where A denotes the vector potential of the excitation, ε the light polarization unit vector, $\langle c | \varepsilon \cdot p | v \rangle$ the interband matrix elements, and $S_{cv}(\hbar\omega)$ the line-shape function of interband exciton. In a 2D system, U_n^l could be described by a solution of 2D Wannier-Mott exciton $U_n^l(\rho, \theta) = \frac{1}{\sqrt{\pi}(n-\frac{1}{2})^{3/2}} \sqrt{\frac{(n-l)!}{(n+l)!}} \left(\frac{2\rho}{n-\frac{1}{2}}\right)^l \exp\left(-\frac{\rho}{n-\frac{1}{2}}\right) L_n^{2l}\left(\frac{2\rho}{n-\frac{1}{2}}\right) \exp(i l \theta)$ and the exciton binding energy could be described as $E_n = \frac{Ry^*}{(n-\frac{1}{2})^2}$ where $n=1, 2, \dots$ is the principle quantum number, $l=0, 1, \dots, (n-1)$ is the angular quantum number, and L_{2n}^l is the associate Laguerre polynomial. As the exciton oscillator strength decays as n^{-3} , only the ground state ($n=1$) and the first two excited states are considered. In a one-photon process, the ground state $1s$ ($n=1, l=0$) dominates; Whereas in a two-photon process the ground state and ns states ($l=0$) are dramatically subsidized owing to $\nabla U_n^l(\rho = 0) \approx 0$ and the p state dominates. Analyzing the difference between one- and two-photon processes would lead to extracting the exciton binding energy of monolayer TMDC.

Figure 3 shows a TP-PLE spectrum of monolayer WS_2 , where the PL intensity of free band-edge exciton A is recorded as a function of the pulsed excitation energy. With the contrasting optical transition strength, two-photon excitation resonant with p type exciton states dominates while s type is nearly invisible. The prominent PL occurs at the excitation around 1.2eV which is

the half of the exciton B energy and 1.29eV. There is a significant gap state in the range of 1.35-1.36eV where the PL intensity drops to nearly negligible. The negligible but nonzero PL intensity likely results from the re-absorption of the second harmonic excitation, since the SHG intensity is more than one order of magnitude higher than that of two-photon luminescence as shown in Figure 3b. Upon the excitation just above the gap ($> 1.365\text{eV}$) as indicated by the arrow in Figure 3a, the PL intensity shows a linear increase with the excitation energy as indicated in the inset. It is the signature of two-photon absorption with in-plane polarization in 2D system[15]. Besides, the two local minimums at higher excitation energy around 1.44eV and 1.46eV have significant PL intensity and therefore are unlikely to be the single-particle band gap state. Thus the single-particle gap could be determined at 2.73eV (2X1.365eV), consistent with Ref[16]. Given that the PL peaks at 2.02eV presenting the energy of the ground-state exciton, the exciton binding energy of $E_b = 0.71 \pm 0.01\text{eV}$ is extracted from the energy difference between the ground-state exciton and the onset of the inter-band continuum.

With the band-edge exciton binding energy of 0.71eV we could attribute the peaks around 2.42eV (2X1.21eV) and 2.58eV (2X1.29eV) in the TP-PL spectrum to the excited states of excitons, which are qualitatively consistent with the recent *ab initio* calculation[16]. As the exciton A and B both originate from the spin-split valence bands at K(K') valley with the similar effective mass, a similar strength of binding energy is expected. Besides, the PL intensity around the peak A' and A'' monotonically decreases. Both peaks are likely to be the excited state of the same exciton, and we tentatively attribute peaks A' and A'' to the $2p$ and $3p$ states of exciton A respectively. The exciton binding energy could also be evaluated from the energy difference between exciton $1s$ and np states. The 2D hydrogen model gives the energy difference between $1s$ and $2p(3p)$

$$E_b = 4Ry^* = \frac{9}{8} \Delta E_{1s-2p} = \frac{100}{96} \Delta E_{1s-3p}$$

which correspond to $E_b = 0.48\text{eV}$ and $E_b = 0.58\text{eV}$ respectively. The alternative assignment for example peak A' to $3p$ state leads to $E_b = 0.45\text{eV}$. These are significantly smaller than $E_b = 0.71 \pm 0.01\text{eV}$ extracted from the energy difference between the ground state exciton and the onset of the inter-band continuum, and the distribution of these excited states also significantly deviates from that of the 2D hydrogen model. The difference may lie in the modification of the 2D hydrogen model by electron-phonon and electron correlation interactions in monolayer TMDC. Recent first principle simulation shows that q-dependent screening dramatically enhances the binding energy of the excited states of excitons[2, 16]. Nevertheless, it is safe to extract the exciton binding energy of $E_b = 0.71 \pm 0.01\text{eV}$ by the energy difference

between $1s$ exciton and the onset of the interband continuum, independent of the assignments of the excited states. It also implies that the model to estimate the exciton binding energy via trion binding energy is inappropriate.

The two-photon absorption has a quadratic dependence on the excitation intensity in principle. The two-photon photoluminescence (TP-PL) intensity from monolayer WS_2 displays a clear quadratic dependence on the excitation intensity at low power as shown in figure 3c. As the excitation intensity increases above $0.2\text{GW}/\text{cm}^2$, the PL intensity experiences a clear transition from quadratic to linear dependence on the excitation intensity. If we follow the simple model

$$\frac{dN}{dt} = \alpha I^2 - \frac{N}{\tau} - \frac{1}{2} \gamma N^2 = 0$$

where N denotes the exciton density, I the excitation intensity, α the two-photon absorption cross section, τ the exciton lifetime and γ the exciton-exciton annihilation rate, the fitting of the quadratic dependence $I_{ph} = \alpha \tau I^2$ ($I \rightarrow 0$) gives two-photon absorption cross section of $\alpha \approx 3.5 - 5.3 \times 10^4 \text{cm}^2 \text{W}^{-2} \text{S}^{-1}$ at 1.59eV where the PL quantum yield of 4×10^{-3} [3] and the exciton lifetime of 100ps are assumed[22]. Subsequently the linear dependence slope at high intensity $\sqrt{\frac{2\alpha}{\gamma}}$ yields the exciton-exciton annihilation rate $\gamma \approx 0.31 - 0.47 \text{cm}^2/\text{s}$ which is qualitatively consistent with that in monolayer MoSe_2 measured by pump-probe reflection spectroscopy[21]. The linear intensity dependence of TP-PL is the evidence of the strong exciton-exciton interactions in monolayer TMDCs.

In summary, the linear absorption spectroscopy cannot resolve the electronic interband transition edge down to 10K due to the strong electron-phonon scattering and the overlap of excitons around Γ point. The TP-PL measurements successfully probe the excited states of the band-edge exciton and the single-particle band gap. The exciton binding energy of $0.71 \pm 0.01\text{eV}$ is extracted by the energy difference between $1s$ exciton and the single-particle gap in monolayer WS_2 . The distribution of the exciton excited states significantly deviates from the 2D hydrogen model. The giant exciton binding energy manifests the unprecedented strong Coulomb interactions in monolayer TMDCs.

* Electronic address: xdcui@hku.hk

- [1] T. Cheiwchanchamnangij and W. R. L. Lambrecht, Physical Review B 85, 205302 (2012).
- [2] D. Y. Qiu, F. H. da Jornada, and S. G. Louie, Physical Review Letters 111, 216805 (2013).
- [3] K. F. Mak, C. Lee, J. Hone, J. Shan, and T. F. Heinz, Physical Review Letters 105, 136805 (2010)

- [4] A. Splendiani, L. Sun, Y. Zhang, T. Li, J. Kim, C.-Y. Chim, G. Galli, and F. Wang, *Nano Letters* 10, 1271 (2010).
- [5] H. Zeng et al., *Sci. Rep.* 3 (2013)
- [6] W. Zhao, Z. Ghorannevis, L. Chu, M. Toh, C. Kloc, P.-H. Tan, and G. Eda, *ACS Nano* 7, 791 (2012).
- [7] H. L. Shi, H. Pan, Y. W. Zhang, and B. I. Yakobson, *Physical Review B* 87, 155304(2013).
- [8] A. Ramasubramaniam, *Physical Review B* 86, 115409 (2012).
- [9] A. A. Mitroglu, P. Plochocka, J. N. Jadczyk, W. Escoffier, G. L. J. A. Rikken, L. Kulyuk, and D. K. Maude, *Phys. Rev. B* 88, 245403(2013)
- [10] J. Bordas, *Some Aspects of Modulation Spectroscopy in Optical and electrical properties* (Springer, 1976), pp. 145.
- [11] K. F. Mak, K. He, C. Lee, G. H. Lee, J. Hone, T. F. Heinz, and J. Shan, *Nat Mater* 12, 207 (2013).
- [12] J. S. Ross et al., *Nat Commun* 4, 1474 (2013).
- [13] A. Thilagam, *Physical Review B* 55, 7804 (1997).
- [14] A. Reina, H. Son, L. Jiao, B. Fan, M. S. Dresselhaus, Z. Liu, and J. Kong. *J. Phys. Chem. C.* 112, 17741 (2008).
- [15] A. Shimizu, T. Ogawa, and H. Sakaki, *Physical Review B* 45, 11338 (1992).
- [16] Z. Ye, T. Cao, K. O'Brien, H. Zhu, X. Yin, Y. Wang, S. G. Louie and X. Zhang, arXiv:1403.5568
- [17] T. Ando, Y. Zheng, and H. Suzuura, *Journal of the Physical Society of Japan* 71, 1318 (2002).
- [18] Z. Gong, G.-B. Liu, H. Yu, D. Xiao, X. Cui, X. Xu, and W. Yao, *Nat Commun* 4 (2013).
- [19] S. Tongay et al., *Nano Letters* 13, 2831 (2013).
- [20] D. Xiao, G.-B. Liu, W. Feng, X. Xu, and W. Yao, *Physical Review Letters* 108, 196802 (2012).
- [21] N. Kumar, Q. Cui, F. Ceballos, D. He, Y. Wang and H. Zhao, arXiv:1311.1079
- [22] B. Zhu, H. Zeng, J. Dai, Z. Gong and X. Cui, arXiv:1403.6224

The work is supported by Area of excellency (AoE/P-04/08), CRF of Hong Kong Research Grant Council and SRT on New Materials of University of Hong Kong